2024 IEEE 15th International Symposium on Power Electronics for Distributed Generation Systems (PEDG) | 979-8-3503-6100-1/24/$31.00 ©2024 IEEE | DOI: 10.1109/PEDG61800.2024.10667407

A Comprehensive Strategy for Grid Forming Control in DC Coupled Photovoltaic and Battery Energy Storage Inverters

1st Houshang Salimian Rizi
Semiconductor Power Electronics Center (SPEC)
The University of Texas at Austin
Austin, USA
salimian@utexas.edu

2nd Zibo Chen
Semiconductor Power Electronics Center (SPEC)
The University of Texas at Austin
Austin, USA
zibochen@utexas.edu

3rd Alex Q. Huang
Semiconductor Power Electronics Center (SPEC)
The University of Texas at Austin
Austin, USA
aqhuang@utexas.edu

4th Pedro Rodriguez
Intelligent Clean Energy Systems
Luxembourg Institute of Science and Technology
Luxembourg
pedro.rodriguez@list.lu

***Abstract*— This paper presents an integrated DC-DC and DC-AC grid-forming control strategy for DC-coupled photovoltaic (PV) plus battery energy storage systems, considering the effect of DC link voltage variations caused by direct PV connections. A power reference algorithm determines power distribution between the PV and battery to the grid while observing device power ratings to prevent the over-rating of components and keep the battery's state of charge within an acceptable range. The simulated utility-scale model in MATLAB/Simulink illustrates its ability against extreme phase angle variation contingencies in the grid while controlled through grid-forming control with a fast dynamic on DC link voltage. The simulation results confirm the effectiveness of the proposed control in integrating PV plus battery configurations with grid forming control and maintaining reliable grid operation under severe grid disturbances.**

Keywords*— battery, boost, control, energy storage, grid forming, inverter, renewable, solar, voltage control.

I. Introduction

The technological advancements in recent decades have resulted in enhancing the efficiency and affordability of renewable sources. In addition, advancements in power semiconductor devices and the power electronics industry have introduced highly efficient power converters with higher control bandwidth that enable integration of renewable energy sources and energy storage systems into the power grid. In recent years by utilizing inverter-based resources (IBRs), the power grid has shifted toward renewable energy sources [1]. The inherently variable nature of solar and wind energy, which is subject to geographic and meteorological influences, introduces novel challenges for grid stability and reliability. The conventional power grid is designed based on a system dominated by synchronous generators that support the grid through frequency and voltage regulation in response to contingencies [2, 3]. With an increasing share of IBRs in energy production, the grid faces new challenges caused by inherent characteristics of traditional IBR controllers. Grid-following control strategies, designed to follow grid voltage in a grid with stable voltage reference, and operate as current sources, cannot provide grid stability in an IBR-dominated grid. This has catalyzed a wave of research into developing advanced grid-forming control strategies, aiming to enhance the stability and reliability of the grid by operating as a voltage-controlled source instead of a current-controlled source [4].

The concept of grid-forming control was initially introduced in microgrids with droop control mechanisms, in which the power sharing between IBRs is set by a droop coefficient that synchronizes their frequency [4]. Building upon this foundation, the grid-forming concept has since been extended to large-scale power grids, starting a new era of grid integration for renewable energy sources. Key advancements in this domain include the development of virtual synchronous generator concepts in the 2000s [5], which emulate the behavior of synchronous generators within microcontrollers and apply it to inverter switching operations. Another notable approach is power synchronized control (PSC), which leverages the power balance equations to synchronize with the grid and operate as a voltage source [6]. Other notable control methods include virtual oscillator control (VOC), utilizing virtual oscillators within microcontrollers to achieve superior dynamics compared to traditional methods [7] and synchronous power controller (SPC) with utilizing virtual admittance method [8].

The overarching goal of research in this area is to endow inverters with grid-forming capabilities, enabling them to perform numerous functions essential for grid stability and grid integration. These functions include facilitating black start capabilities, autonomously synchronizing with the grid, providing frequency support following contingency events, offering reactive power support, handling faults effectively, and operating seamlessly under unbalanced conditions [9, 10]. By designing inverters with these capabilities, researchers aim to

This material is based upon work supported by the U.S. Department of Energy's Office of Energy Efficiency and Renewable Energy (EERE) under the Solar Energy Award Number DE-EE0010651.

support the resilience and flexibility of power grids in the face of increasing renewable energy penetration. In this regard, in addition to power controllers to achieve grid forming capabilities extensive research on the inner control loops of inverters have been done to ensure small signal stability of grid forming inverters in weak and stiff grids [11]. Therefore, in addition to conventional voltage and current controllers virtual impedance and virtual admittance [12] are used to increase stability of the grid forming inverter and provide other capabilities such as short circuit limiting with fast dynamic [13].

Solar PV annual added capacity in the power grid has gone through significant growth in the past decade. Additionally, solar plus battery energy storage is a new trend in recent years, emphasizing the shift toward enhanced grid stability and reliability [14-16]. However, research on integrating grid-forming control with these systems is less studied, identifying a significant gap in the field. Most studies focus on grid-forming inverters with stable DC link voltages, i.e., connecting the DC link to battery energy storage, neglecting the variations in DC link voltage. In [17], the effect of DC voltage dynamics is modeled and considered in the grid-forming control in addition to other input variables. A few studies have proposed power curtailment strategies to manage PV without storage systems, providing an energy buffer through not operating at the PV's maximum power point [18]. These methods sacrifice potential energy production and neglect the benefits of direct energy storage and PV integration. Existing studies primarily focus on grid-following control of PV inverters coupled with energy storage, often overlooking the potential and challenges of combining PV generation with grid-forming control. PV plus storage inverters can be categorized based on the coupling point of energy storage and PV: AC coupled and DC coupled. AC-coupled configurations offer more flexibility by processing power in two independent converters. This allows the use of well-developed grid-following control for PV inverters and grid-forming control for energy storage with stable DC link voltage, as shown in [19], simplifying the grid-forming control of these converters. However, using extra hardware in this solution adds to the complexity, increases the price, and lowers the overall efficiency of the system [20]. Therefore, a gap exists in applying grid-forming technology. The two most common topologies for DC-coupled PV plus battery systems are PV-centric and battery-centric configurations. In the PV-centric solution, the PV panel directly connects to the inverter's DC link, and the battery connects to the DC link through a DC-DC conversion stage. In the battery-centric approach, the battery is linked directly to the DC link of the inverter, and the PV system is connected to the DC link through a DC-DC conversion stage. The PV-centric solution is more efficient for transferring power from PV to the grid, while the battery-centric approach is optimal for exchanging power between the energy storage and the grid with lower number of conversion stages [21].

17, 19, 21读

This paper seeks to explore the gaps identified by undertaking a thorough analysis of grid-forming control within DC-coupled PV and battery energy storage systems. Initially, it outlines the model of the configuration under consideration. Then, the grid-forming control for this specific setup is introduced, with a particular focus on the implications of DC link voltage fluctuations. Furthermore, a power reference algorithm designed to regulate power flow from each segment is presented. The paper concludes with simulation results for a 1.4MW PV system to substantiate the efficacy of the introduced control strategy for the described configuration.

II. DC Coupled PV and Battery System Configuration

For the outlined configuration aimed at utility-scale applications, the primary objective is ensuring the injection of maximum power from PV into the grid. However, since power generation is contingent upon solar irradiation, which often falls below the system's rated power generation for many hours of the day, the inverter's rated power is set lower than that of the PV system. Any surplus power generated by the PV system can be stored in the battery energy storage system. Due to both configuration needs and financial considerations, the ratings for the DC-DC converter and the energy storage system are typically set below that of the inverter, e.g. DC-DC rated power is 40% of inverter rated power. For utility-scale applications, the typical open-circuit voltage for PV systems is 1500V. The configuration proposed in Fig. 1 is suitable for such applications. It consists of two stages: the first stage is connecting the battery to the DC link via a boost converter, followed by converting DC to AC using a three-phase inverter. Averaging across one inverter switching cycle yields the following equations:

$$d\frac{V_{cd}}{dt} = \frac{I_{fd}}{C_f} - \frac{I_{gd}}{C_f} + \omega_e V_{cq} \quad (1)$$

$$d\frac{V_{cq}}{dt} = \frac{I_{fq}}{C_f} - \frac{I_{gq}}{C_f} - \omega_e V_{cd} \quad (2)$$

$$d\frac{I_{fd}}{dt} = \frac{d_d.V_{PV}}{L_f} - \frac{V_{cd}}{L_f} + \omega_e I_{fq} \quad (3)$$

$$d\frac{I_{fq}}{dt} = \frac{d_q.V_{PV}}{L_f} - \frac{V_{cq}}{L_f} - \omega_e I_{fd} \quad (4)$$

$$d\frac{I_{gd}}{dt} = \frac{V_{cd}}{L_g} - \frac{V_{gd}}{L_g} + \omega_e I_{gq} \quad (5)$$

$$d\frac{I_{gq}}{dt} = \frac{V_{cq}}{L_g} - \frac{V_{gq}}{L_g} - \omega_e I_{gd} \quad (6).$$

These equations convert quantities from the abc to the dq0 frame, where V_{cd} and V_{cq} denote output filter capacitor voltages, I_{fd} and I_{fq} are output inductive filter currents, I_{gd} and I_{gq} represent grid currents, V_{PV} is inverter's DC link voltage, and d_d and d_q are the inverter's modulation indices for the d-frame and q-frame, respectively. The boost stage equations in continuous current mode, described by:

$$d\frac{V_{PV}}{dt} = \frac{(1-d_b)I_{Lb}}{C_{PV}} + \frac{I_{PV}}{C_{PV}} - \frac{d_d.I_d}{C_{PV}} - \frac{d_q.I_q}{C_{PV}} \quad (7)$$

$$d\frac{I_{Lb}}{dt} = \frac{V_{bat}}{L_b} - \frac{(1-d_b)V_{PV}}{L_b} \quad (8)$$

where d_b is duty cycle of bottom switch, I_{Lb} is the current through the boost inductor, and V_{bat} is the battery voltage. Equations (3), (4), and (7) highlight the coupling between the AC and DC circuits, demonstrating that the DC link voltage is influenced by AC power, battery power, and PV current.

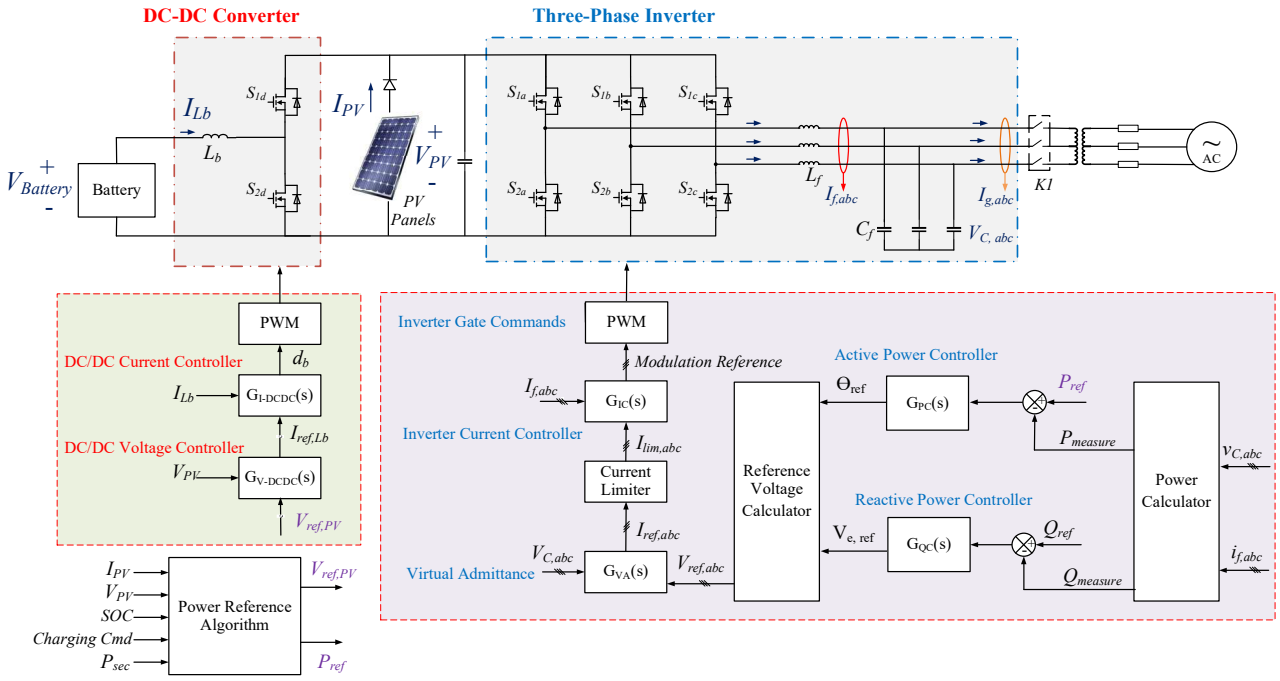

Fig. 1. DC Coupled PV plus battery energy storage configuration.

III. Proposed Grid Forming Control of DC Coupled PV and Battery Inverter

The design of the proposed controller is divided into two interconnected segments. The DC-DC and DC-AC controllers are linked through the DC link voltage reference for the DC-DC controller and the power reference for the DC-AC controller, both of which are established by the power reference algorithm.

A. DC-DC Controller

The DC-DC controller, shown in Fig. 2(a), features a cascaded architecture with voltage and current control loops, each regulated by proportional-integral (PI) controllers. This controller is designed to respond with the highest bandwidth within the control system, ensuring the DC link voltage remains stable amidst significant disturbances from the AC grid or fluctuations in PV generation.

B. DC-AC Controller

The DC-AC controller, depicted in Fig. 2(b), employs a power synchronization loop with a PI controller for setting the active power by generating the reference phase angle for grid synchronization. A droop coefficient (D_p) can be added to facilitate primary frequency response or power sharing within a microgrid. Moreover, reactive power management adjusts the voltage magnitude of the inverter for volt-var control. This controller integrates virtual admittance (A_v) to derive the inverter's current reference for the internal current control loop:

$$A_v = \frac{1}{sL_v + R_v} \qquad (9).$$

Here, L_v and R_v represent the virtual inductance and resistance, respectively. This approach, favoring virtual admittance over

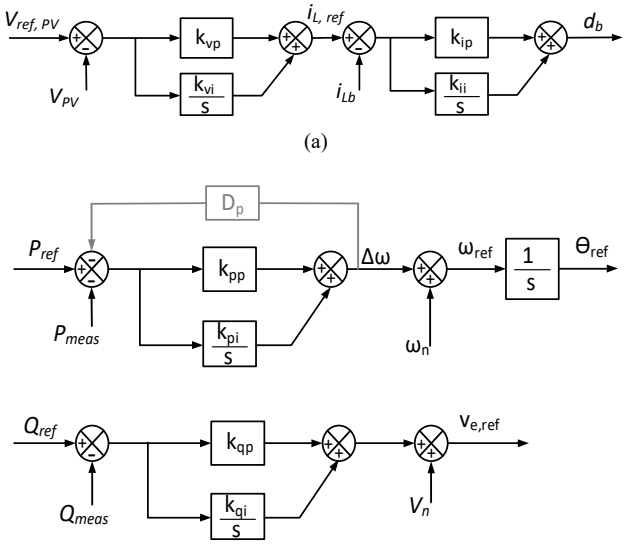

Fig. 2. a) DC-DC cascaded controller b) PSC for gird forming control of DC-AC controller.

virtual impedance, reduces the noise associated with the derivative term in virtual impedance [9]. Small signal analysis has demonstrated that virtual admittance ensures reliable stability in grids, regardless of their short circuit ratio (SCR) values [11].

C. Power Reference Algorithm

This section introduces a power reference algorithm, shown in Fig. 3, that synchronizes the DC-DC and DC-AC controllers

to ensure efficient power transfer from PV to the grid. Assuming negligible power losses in the system, the power balance equation is presented as

$$P_{AC} = P_{PV} + P_{bat} \quad (10).$$

Thus, by defining the power reference for the AC side, the power from the battery can be appropriately regulated. The proposed algorithm incorporates several constraints, adhering to the following hierarchy:

- Protecting the inverter and converter by capping the power transfer at each stage to their respective rated capacities, $P_{rated,inv}$ and $P_{rated,\ boost}$, respectively.
- Protecting the converter against DC link voltage variations caused by contingencies in the grid.
- Monitoring the battery's state of charge (SOC) and adjusting charging commands to prevent overcharging or deep discharging by P_{SOC}.
- Allocating any excess power as per the directives of higher-level control (P_{sec})
- Maximizing power generation from the PV (P_{PV}) through the implementation of the MPPT algorithm.
- Employing a flexible power point tracking (FPPT) when P_{MPP} exceeds the combined rated power of the battery and inverter.

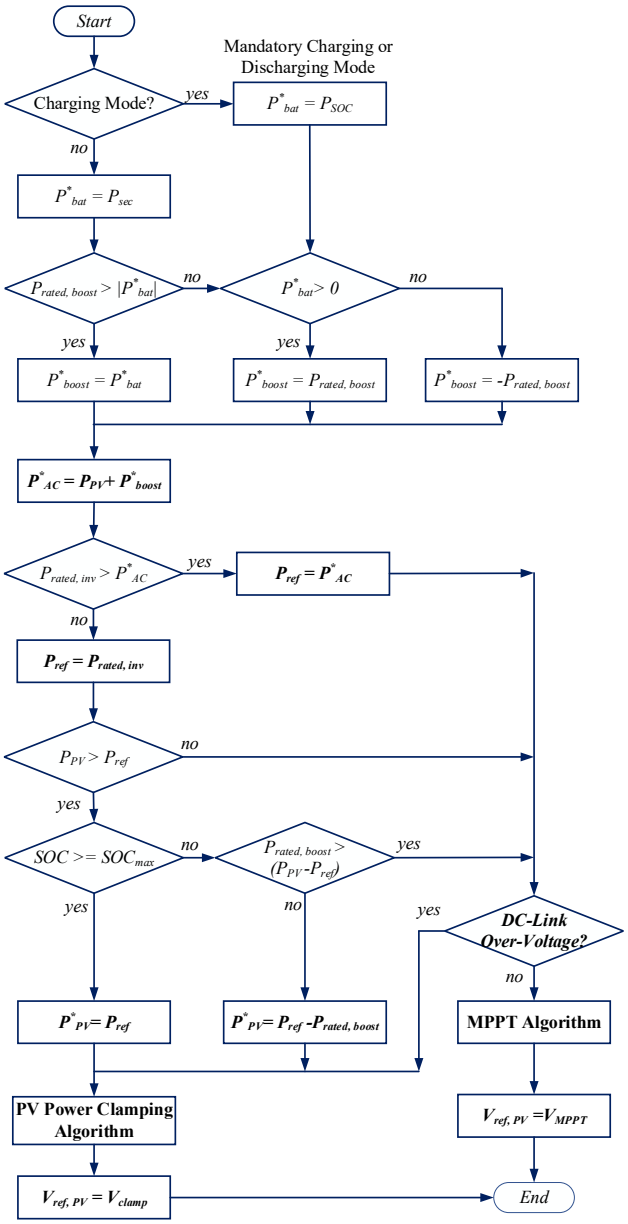

Fig. 3. Porposed power reference algorithm for setting power refence

In Fig. 4(a), the power-voltage (P-V) curve of a sample inverter, with a 1500V open-circuit voltage, is depicted at a temperature of 30°C. In Fig. 4, all power values are normalized, with the base power defined as ($P_{rated,inv}$) and the maximum power from the PV system under 100% sun irradiance is represented as 1.4 per

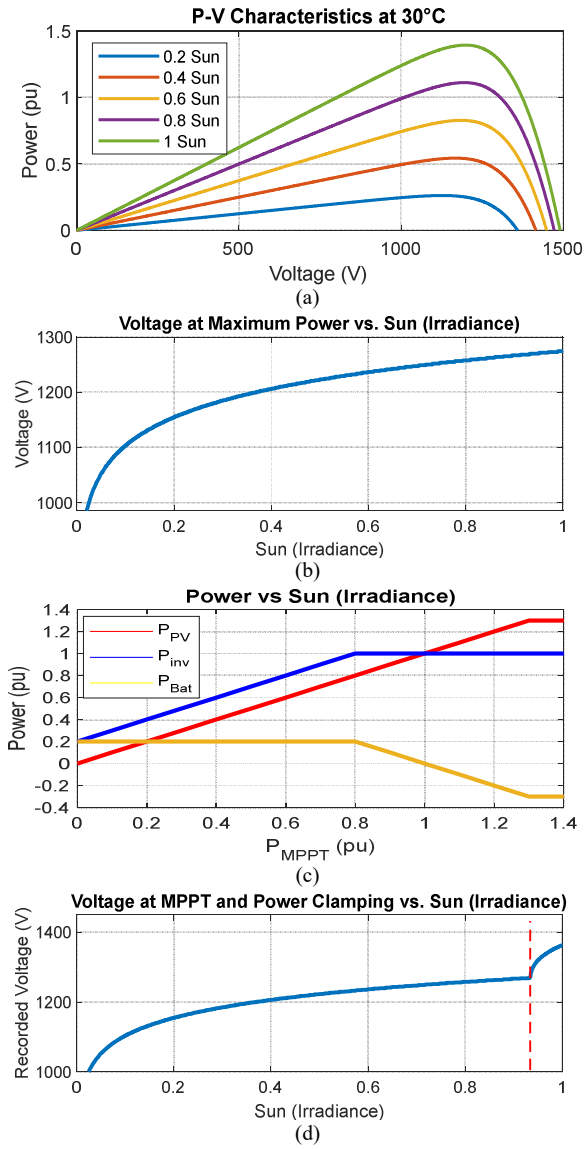

Fig. 4. A sample PV characteristic. a) P-V curve at T = 30°C b) Voltage at maximum power. c) Inverter, PV, and battery power after implementing power reference algorithm. d) DC link voltage reference with MPP and power clamping.

unit (pu). Fig. 4(b) illustrates that the V_{PV} required to reach the maximum power point varies with solar irradiance. The outcomes of applying the algorithm are presented in Figs. 4(c) and 4(d). Specifically, Fig. 4(c) demonstrates that when $P_{rated, boost}$ is set to 0.3 pu and operates in normal mode, it is capable of both charging and discharging. The higher-level control issues a command (P_{sec}) to add an additional 0.2 pu from the battery to the grid power, on top of the power generated by the PV. The battery contributes 0.2 pu to the grid for PV power generation levels from 0 to 0.8 pu. As the inverter approaches $P_{rated, inv}$, the contribution from the battery decreases to maintain the inverter's power within safe limits. Once PV power exceeds 1 pu, the battery begins to charge, storing excess PV generation. However, since the boost rated power is 0.3 pu, the system exits MPPT algorithm and initiates a power clamping algorithm to safeguard the battery and inverter once PV power reaches 1.3 pu, hence generating power slightly below the optimal point. Fig. 4(d) shows the reference voltage for the inverter's DC link, where MPPT is applied up to a PV power of 1.3 pu. Beyond this point, from 1.3 to 1.4 pu, the power clamping algorithm takes over, resulting in the PV voltage exceeding the maximum power point voltage (V_{clamp}).

IV. Simulation Results

The performance of a utility-scale grid-forming system is verified through simulation results in MATLAB/Simulink, highlighting its grid-forming capabilities and power reference algorithm. The system, designed to connect to a three-phase 34kV 60Hz grid via a step-up transformer and a 5-mile π-model line, incorporates an inverter outputting 600V. With a switching frequency set at 8kHz and equipped with an output LC filter consisting of 80μH inductance and 200μF capacitance, the system comprises a 1MW inverter and a PV system that reaches up to 1.4MW maximum output at an open circuit voltage of 1500V, alongside a battery and boost converter each rated at 400kW.

In Fig. 5, the simulation results illustrate the system's adeptness in maintaining stability and grid synchronization under challenging scenarios. Specifically, in Fig. 5(a), the system's handling of a 30° phase angle jump in grid voltage at t = 2s demonstrates the inverter's capacity for current limitation and swift DC link voltage recuperation, followed by successful re-synchronization with the grid after the disturbance. Post-phase jump, there is a temporary drop in PV voltage, which quickly stabilizes back to the Maximum Power Point Voltage (VMPP) within two cycles. Concurrently, the grid-forming power controller promptly adjusts to the grid's frequency, evidencing the system's resilience and robustness in managing grid perturbations. During stable operation, the system efficiently manages energy production, using 200kW of excess power to charge the battery while directing 1MW into the grid.

Similarly, in Fig. 5(b), a -30° balanced phase jump occurs in the grid at t = 2.4s. The severity of the DC link voltage variation

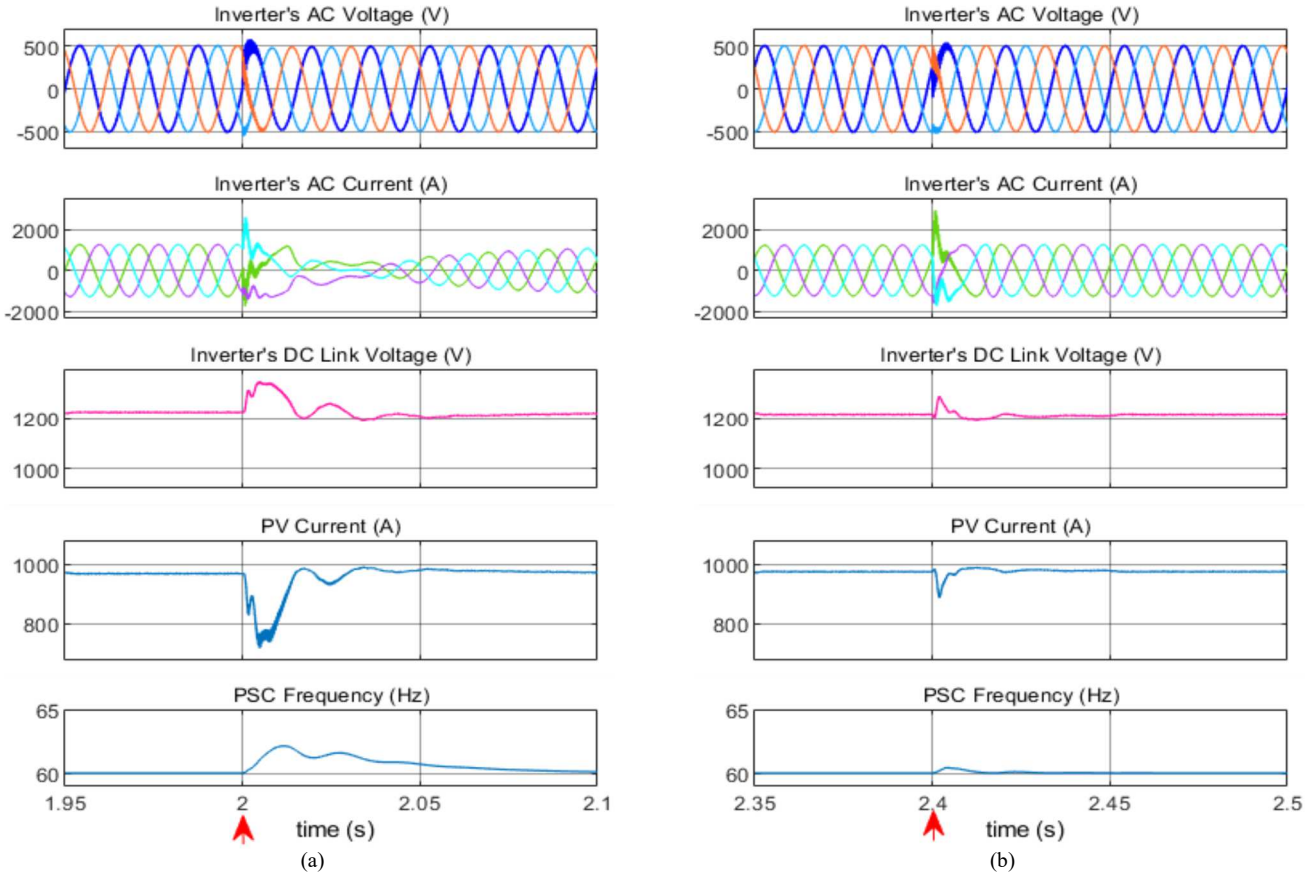

Fig. 5. DC coupled PV and battery system response after a balanced phase angle jump in the grid voltage; (a) 30º phase jump at t=2s (b) -30º phase jump at t=2.4s.

is less as power flows from the inverter to the grid due to the leading voltage, allowing the system to synchronize with the grid faster. In the first case, the overvoltage in DC link voltage is limited because of the power reference algorithm, which limits the DC link voltage by using FPPT to clamp the PV power to open-circuit PV power and limit the power transferred from the battery. The frequency is also increased to synchronize with the grid and reduce the phase angle difference between the grid and PV inverter.

V. Conclusions

This paper has introduced and validated an integrated grid-forming and DC-DC control strategy for the efficient integration of DC-coupled PV and battery energy storage systems into power grids. By implementing a power reference algorithm, the strategy ensures optimal energy distribution between the PV array, grid, and battery storage, capitalizing on renewable energy while respecting the power ratings of individual components to prevent overloading. This approach not only maximizes the utility of renewable sources but also maintains the system's operational integrity within its constraints. The utility-scale simulation model, validated in MATLAB/Simulink, is characterized by a 34kV voltage level and a 1.4MW power rating, demonstrating the system's robustness in managing extreme phase angle jump contingencies. This capability underscores the system's resilience and reliability, which are critical for the stable operation of power grids with high penetrations of renewable energy.

References

[1] Z. Tang, Y. Yang and F. Blaabjerg, "Power electronics: The enabling technology for renewable energy integration," in *CSEE Journal of Power and Energy Systems*, vol. 8, no. 1, pp. 39-52, Jan. 2022.

[2] H. Laaksonen, "Universal Grid-Forming Method for Future Power Systems," in IEEE Access, vol. 10, pp. 133109-133125, 2022.

[3] H. S. Rizi, T. Chen and A. Q. Huang, "A Novel Power Flow Controller for Behind the Meter Demand Response," *2023 IEEE Energy Conversion Congress and Exposition (ECCE)*, Nashville, TN, USA, 2023, pp. 2466-2472, doi: 10.1109/ECCE53617.2023.10362266.

[4] R. Rosso, X. Wang, M. Liserre, X. Lu and S. Engelken, "Grid-Forming Converters: Control Approaches, Grid-Synchronization, and Future Trends—A Review," in *IEEE Open Journal of Industry Applications*, vol. 2, pp. 93-109, 2021, doi: 10.1109/OJIA.2021.3074028.

[5] H.-P. Beck and R. Hesse, “Virtual synchronous machine,” in Proc. 9th Int. Conf. Elect. Power Qual. Utilization, Oct. 2007, pp. 1–6.

[6] S. D’Arco and J. A. Suul, “Virtual synchronous machines classification of implementation and analysis of equivalence to droop controllers for microgrids,” in Proc. IEEE PowerTech, 2013, Grenoble, France, Jun. 2013, pp. 1–7.

[7] M. Colombino, D. Groß, J. Brouillon, and F. Dörfler, “Global phase and magnitude synchronization of coupled oscillators with application to the control of grid-forming power inverters,” IEEE Trans. Autom. Control, vol. 64, no. 11, pp. 4496–4511, Nov. 2019.

[8] A. Tarrasó, J. I. Candela, J. Rocabert and P. Rodriguez, "Grid voltage harmonic damping method for SPC based power converters with multiple virtual admittance control," *2017 IEEE Energy Conversion Congress and Exposition (ECCE)*, Cincinnati, OH, USA, 2017, pp. 64-68, doi: 10.1109/ECCE.2017.8095762.

[9] H. Wu and X. Wang, "Control of Grid-Forming VSCs: A Perspective of Adaptive Fast/Slow Internal Voltage Source," in *IEEE Transactions on Power Electronics*, vol. 38, no. 8, pp. 10151-10169, Aug. 2023.

[10] H. S. Rizi, Z. Chen, E. Nazerian, W. Xu and A. Q. Huang, "Solid State Condenser (SSC) - A New FACTS Device for Grid Inertia Support," *2023 IEEE Texas Power and Energy Conference (TPEC)*, College Station, TX, USA, 2023, pp. 1-6, doi: 10.1109/TPEC56611.2023.10078567.

[11] L. Huang, C. Wu, D. Zhou and F. Blaabjerg, "Impact of Virtual Admittance on Small-Signal Stability of Grid-Forming Inverters," *2021 6th IEEE Workshop on the Electronic Grid (eGRID)*, New Orleans, LA, USA, 2021, pp. 1-8, doi: 10.1109/eGRID52793.2021.9662150.

[12] J. D. V. Leon, A. Tarraso, J. I. Candela, J. Rocabert and P. Rodriguez, "Grid-Forming Controller Based on Virtual Admittance for Power Converters Working in Weak Grids," in *IEEE Journal of Emerging and Selected Topics in Industrial Electronics*, vol. 4, no. 3, pp. 791-801, July 2023.

[13] B. Fan, T. Liu, F. Zhao, H. Wu and X. Wang, "A Review of Current-Limiting Control of Grid-Forming Inverters Under Symmetrical Disturbances," in *IEEE Open Journal of Power Electronics*, vol. 3, pp. 955-969, 2022.

[14] C. Chen, Z. Chen, H. S. Rizi and A. Q. Huang, "Comparative Study of 100kW Three-Level Bidirectional DC-DC Converters for Battery Storage Integration with 1500V PV Inverter," *2023 IEEE Applied Power Electronics Conference and Exposition (APEC)*, Orlando, FL, USA, 2023, pp. 3061-3068, doi: 10.1109/APEC43580.2023.10131202.

[15] M. Mohammadi and J. Thornburg, "Strategic EV Charging and Renewable Integration in Texas," *2024 IEEE Texas Power and Energy Conference (TPEC)*, College Station, TX, USA, 2024, pp. 1-6, doi: 10.1109/TPEC60005.2024.10472168.

[16] E. Nazerian, R. Yu, Q. Huang, M. Heydari, H. S. Rizi and A. Q. Huang, "High Efficiency, High Power Density 10kW Flying Capacitor Converter Based on 650V GaN for 800V EV Applications," *2023 IEEE Energy Conversion Congress and Exposition (ECCE)*, Nashville, TN, USA, 2023, pp. 1863-1869, doi: 10.1109/ECCE53617.2023.10362881.

[17] L. Zhao, Z. Jin and X. Wang, "Small-Signal Synchronization Stability of Grid-Forming Converters With Regulated DC-Link Dynamics," in *IEEE Transactions on Industrial Electronics*, vol. 70, no. 12, pp. 12399-12409, Dec. 2023.

[18] Z. Chen, R. H. Lasseter and T. M. Jahns, "Active Power Reserve Control for Grid-Forming PV Sources in Microgrids using Model-based Maximum Power Point Estimation," *2019 IEEE Energy Conversion Congress and Exposition (ECCE)*, Baltimore, MD, USA, 2019, pp. 41-48

[19] X. Quan *et al*., "Photovoltaic Synchronous Generator: Architecture and Control Strategy for a Grid-Forming PV Energy System," in *IEEE Journal of Emerging and Selected Topics in Power Electronics*, vol. 8, no. 2, pp. 936-948, June 2020, doi: 10.1109/JESTPE.2019.2953178.

[20] Z. Chen, H. S. Rizi, W. Xu, R. Yu and A. Q. Huang, "Hardware Design of a 150kW/1500V All-SiC Grid-forming Photovoltaic Synchronous Generator (PVSG)," *2022 IEEE Applied Power Electronics Conference and Exposition (APEC)*, Houston, TX, USA, 2022, pp. 1977-1984.

[21] W. Xu, Z. Guo, A. Vetrivelan, R. Yu and A. Q. Huang, "Hardware Design of a 13.8-kV/3-MVA PV Plus Storage Solid-State Transformer (PVS-SST)," in *IEEE Journal of Emerging and Selected Topics in Power Electronics*, vol. 10, no. 4, pp. 3571-3586, Aug. 2022, doi: 10.1109/JESTPE.2021.308

AC coupled